Energies, intensities, and polarizations of channeling radiation in the axial-to-planar channeling transition region

R. W. Dougherty
Code 6693, U.S. Naval Research Laboratory, Washington, D.C. 20375-5345

J. B. Langworthy
8303 Rambler Drive, Adelphi, Maryland 20783

A. W. Sáenz
Department of Physics, Catholic University of America, Washington, D.C. 20064
and Naval Research Laboratory Washington, D.C. 20375-5345
(Received 8 June 1995; revised manuscript received 10 December 1996)

We have investigated numerically the energies, intensities, and polarizations of channeling radiation (CR) photons emitted by relativistic electrons traversing Si and Ni crystals in the transition region from axial to planar channeling. Our work is based on the two-dimensional continuum model commonly used to describe axial channeling in crystals; it is a detailed numerical study of these CR properties embracing this entire region. More specifically, we calculated these properties of CR from 4-MeV electrons in Si as they underwent the transition from axial channeling along the ⟨110⟩ direction to planar channeling by the (100) planes, and in Ni in the transition from axial channeling along this direction to planar channeling by the (001) planes. The two-dimensional model correctly reproduces the experimentally observed planar CR photon energies in both cases, and also correctly predicts that the planar CR is plane polarized. In the transition region, our calculations predict the occurrence of complicated irregular oscillations of the photon energies corresponding to the strongest radiative transitions, and predict even larger oscillations of the intensities of such transitions. This oscillatory behavior could possibly be detected experimentally. [S1050-2947(97)06104-0]

PACS number(s): 61.85.+p, 41.60.−m, 12.20.Ds

I. INTRODUCTION

Pure axial and pure planar channeling radiation (CR) from relativistic electrons traversing crystals is now well understood experimentally and theoretically [1–3]. Much less is known about the CR emitted by such electrons in the angular region where the transition from axial-to-planar channeling is observed to take place. In the present paper, we will study theoretically in a comprehensive quantitative manner the emergence of the planar CR regime in two typical cases. Comparisons with experiment will be made and predictions about this transition that are interesting candidates for experimental investigation will be pointed out.

Very few investigations of CR have been carried out in the axial-to-planar transition region. The subject was first studied experimentally by Anderson *et al.* [3] using 4-MeV electrons incident on Ni. In addition, they investigated it theoretically on the basis of a two-dimensional continuum model of the crystal potential, both qualitatively by means of perturbation theory and quantitatively by the ''many-beam'' formalism [4]. In spite of the fact that they only used 81 beams to calculate the energies of CR photons from 4-MeV electrons in Ni undergoing this transition, the results of their calculations agree well with experiment. No theoretical results on the intensity of CR in this region are presented in Ref. [3]. More recently, the behavior of CR in the transition region was investigated experimentally by Diedrich *et al.* [5] for 72.5-MeV electrons incident on Si [5] and, in particular, for 6.8-MeV electrons incident on diamond [6]. The complexity of the 72.5-MeV data entails that its quantitative theoretical interpretation will be difficult, but the 6.8-MeV data should be readily comparable with the predictions of the present theory.

It is well known that in calculations of electron channeling states and of the accompanying CR it is unnecessary to use the complete three-dimensional crystal potential if the electron of interest is incident on a crystal in a direction sufficiently close to that of a major axis. Indeed, in traversing a crystal such an electron ''sees'' an effective crystal potential that is averaged along this axis [7], and that therefore only exerts a force on the electron in a plane perpendicular to the axis. This is the two-dimensional periodic potential used in Ref. [3] and in the present work, and the corresponding continuum crystal model is sometimes called the ''harp'' model [8]. The strings of the harp are obtained by replacing the atomic strings parallel to the crystal axis in question by continuous, uniformly charged lines that generate the above averaged potential. In the context of this model, one can accurately represent each electronic state populated by the incident plane-wave electron state by a simple approximate solution of the Dirac equation. The solution has the form of a product of a plane wave, describing free relativistic motion in a direction parallel to the crystal axis, and a four-component spinor, describing nonrelativistic motion in the plane perpendicular to this direction. The spinor is completely specified by a two-dimensional Bloch function, which is an eigenstate of a suitable nonrelativistic Hamiltonian [9] (see Sec. II). These eigenstates and the corresponding energy eigenvalues (transverse eigenstates and eigenvalues) are most accurately determined numerically by the many-beam approach. In the present work, we used re-

sults of such numerical calculations, together with formulas derived by standard methods of quantum electrodynamics, to compute the energies, intensities, and polarizations of photons emitted in spontaneous transitions between electronic states described by these solutions of Dirac's equation. By definition, CR is the radiation emitted when such transitions take place between transversely ''bound'' electronic states, i.e., solutions of Dirac's equation that correspond to Bloch eigenfunctions of the above two-dimensional nonrelativistic Hamiltonian belonging to narrow energy bands (see, e.g., Refs. [9–12]).

More specifically, we used the above many-beam approach to calculate the three mentioned properties of CR photons emitted by electrons traversing Si and Ni crystals in directions that encompass the entire transition region from axial to planar channeling. In these calculations, the energy of the incident electrons was taken to be the same as that used in the experiments on CR from Si [2] and Ni [3] in order to compare our results with experiment at an electron energy at which the pertinent CR spectra are fairly simple, thus facilitating their theoretical interpretation. In general, there is good agreement between our results and the experimental findings of Ref. [3]. In addition, our computations predict the presence of rapid irregular oscillations of photon energy and intensity in the transition region, as well as polarization phenomena that would be interesting to investigate experimentally.

The organization of this paper is as follows. In Sec. II we describe the theoretical basis of our approach, while in Sec. III we present and discuss the results of our numerical calculations of the stated properties of CR in the axial-to-planar transition region and compare them with experiment. Our conclusions are summarized in Sec. IV.

II. THEORY

Let x,y,z be a right-handed Cartesian coordinate system, with the z axis parallel to a major axis of the crystal of interest and with the x,z plane parallel to a major crystal plane. The crystal is supposed to be a slab whose faces are parallel to the x,y plane. An electron with momentum $\mathbf{p}$ almost parallel to the z direction is assumed to be incident on the crystal. The direction of $\mathbf{p}$ with respect to the crystal is determined by the angles ϕ and ψ, where ϕ is the angle between the z axis and the orthogonal projection of $\mathbf{p}$ on the x,z plane and ψ the angle between $\mathbf{p}$ and this projection (see Fig. 1). For symmetry reasons, we need only (and will only) consider positive values of ϕ and ψ. If both ϕ and ψ are small (say, less than 10 mrad), then the electron will undergo axial channeling in the z direction, in which case its wave function will be concentrated near the atomic strings parallel to this direction [13]. If ϕ is large but ψ remains small, then the component of $\mathbf{p}$ perpendicular to z is too large to permit axial channeling. In this case, the electron will ''see'' an effective crystal potential that is averaged over the x,z plane, i.e., a one-dimensional periodic potential depending only on y. One then says that the electron is channeled by the atomic planes parallel to the x,z plane. In this situation, it is possible for the electron to be transversely ''bound'' to these atomic planes, in the sense that its wave function is concentrated in their vicinity [14]. For the examples considered here, our calculations demonstrate that the transition from axial to planar channeling takes place as ϕ varies from small to large values with ψ kept fixed [15].

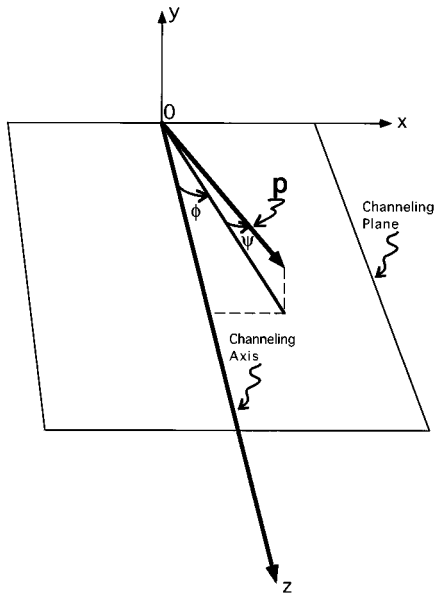

FIG. 1. Channeling geometry.

As mentioned in Sec. I, the transverse electronic eigenstates and eigenvalues needed to calculate the CR emitted by relativistic electrons traversing Si and Ni crystals were determined numerically for the harp potential by means of the many-beam method [4]. We elected to use this approach because it allows one to study the entire transition region without making questionable approximations or using perturbation theory. The basic physical reason why it does is that the harp potential contains in principle all the information needed to determine the properties of the radiation of interest for values of ϕ corresponding to this region.

We will assume that the z axis is parallel to the $\langle 110\rangle$ direction in the cases of Si and Ni. In the former (latter) case, the x,z plane is taken to be parallel to the (110) [(100)] plane and the incident electron momentum is assumed to be almost parallel to the z axis. The points at which the harp strings (averaged atomic strings) parallel to $\langle 110\rangle$ intersect the xy plane form a rectangular Bravais lattice in both crystals, there being 4 sites per unit cell for Si [Fig. 2(a)] and 2 sites per unit cell for Ni [Fig. 2(b)]. If we denote the side length of the unit cell along the x axis by a and that along the y axis by b, then $a=5.431$ and 3.524 Å for Si and Ni, respectively, and $b=2^{1/2}a$ in both cases. Note that for the small values of ϕ and ψ of interest in this paper, $p_x \cong \phi p$, $p_y \cong \psi p$.

The electronic wave function $\Psi(\mathbf{r})$ of a channeled electron is taken to be a four-component spinor that is a solution of the Dirac equation appropriate to the pertinent harp-model potential. Since the potential used in our calculations is very small in absolute value in comparison with the energy of the incident electron, $\Psi(\mathbf{r})$ is well approximated by the following expression [9,16,17]:

$$\Psi(\mathbf{r}) = L^{-1/2}\left(\frac{E_\parallel + m}{2E_\parallel}\right)^{1/2}\begin{pmatrix} u\chi \\ \dfrac{\boldsymbol{\sigma}\cdot\mathbf{p}u}{E_\parallel + m}\chi \end{pmatrix}\exp(ip_z z) \qquad (1)$$

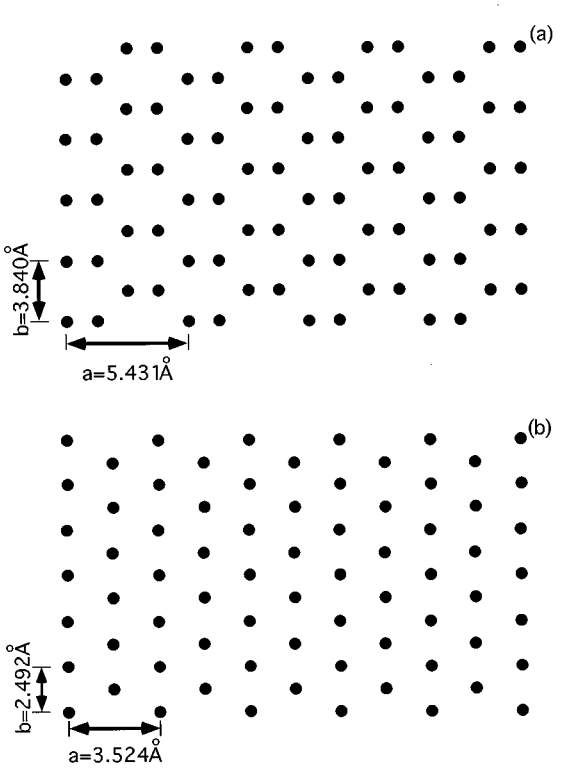

FIG. 2. The dots in parts (a) and (b) depict the intersection of the harp strings with the x,y plane for Si and Ni, respectively. For both crystals, $z\|\langle 110\rangle$.

inside the crystal, which we assume to be a slab of thickness L with sides perpendicular to the z axis. Here $\mathbf{r}=(x,y,z)$; $E_\|=(p_z^2+m^2)^{1/2}$, with p_z the z component of the momentum vector of the incident electron and m its rest mass; $\boldsymbol{\sigma}=(\sigma_x,\sigma_y,\sigma_z)$ is a vector whose components are the Pauli spin matrices; $\tilde{\mathbf{p}}=(-i\nabla_\perp,p_z)$, the subscript $\perp$ denoting a component of the gradient orthogonal to the z axis; and χ is $\binom{1}{0}$ or $\binom{0}{1}$ depending on whether the spin is parallel or antiparallel to this axis. Moreover, $u=u(x,y)$ is the transverse electronic wave function, which is a two-dimensional Bloch function satisfying the nonrelativistic Schrödinger equation

$$\frac{-1}{2m\gamma}\left(\frac{\partial^2}{\partial x^2}+\frac{\partial^2}{\partial y^2}\right)u(x,y)+\overline{V}(x,y)u(x,y)=E_\perp u(x,y) \qquad (2)$$

for a particle with transverse energy $E_\perp$ and relativistic mass $m\gamma$ instead of the usual electronic rest mass m. In Eq. (2), $V(x,y)$ is the two-dimensional harp-model potential, obtained by averaging over the z axis the thermally averaged three-dimensional electron-crystal potential $V(x,y,z)$. We assume that $V(x,y,z)$ consists of a sum of thermally averaged two-body potentials describing the interaction of the electron with the individual atoms of the crystal of interest. More precisely, each two-body potential is a convolution of a Doyle-Turner potential [18] with a Gaussian whose Fourier transform is a suitable Debye-Waller factor [2,3]. The purpose of this thermal averaging is to take account of the thermal motions of the atoms in a phenomenological manner. To solve Eq. (2), we expand $V(x,y)$ in a Fourier series:

$$\overline{V}(\mathbf{r}_\perp)=\sum_{\mathbf{G}\in\Lambda} V_{\mathbf{G}}\exp(i\mathbf{G}\cdot\mathbf{r}_\perp), \qquad (3)$$

where $\mathbf{r}_\perp=(x,y,0)$ and the set Λ over which the sum ranges consists of all vectors $\mathbf{G}=(G_x,G_y,0)$ in the x,y plane such that

$$G_x=\frac{2\pi m_1}{a}, \quad G_y=\frac{2\pi m_2}{b}, \qquad (4)$$

m_1,m_2 being integers. We index the Bloch functions u in Eq. (2) by $\mathbf{p}_\perp=(p_x,p_y,0)$, the quasi-momentum in the periodic zone scheme [19], and expand them in a Fourier series:

$$u_{\mathbf{p}_\perp}(\mathbf{r}_\perp)=\sum_{\mathbf{G}\in\Lambda} C_{\mathbf{p}_\perp}(\mathbf{G})\exp[i(\mathbf{p}_\perp+\mathbf{G})\cdot\mathbf{r}_\perp]. \qquad (5)$$

Inserting Eqs. (3) and (5) into Eq. (2) and equating the coefficients of the relevant exponential factors, the latter equation can be expressed as an infinite-dimensional eigenfunction-eigenvalue problem:

$$M_{\mathbf{p}_\perp}C_{\mathbf{p}_\perp}=E_\perp(\mathbf{p}_\perp)C_{\mathbf{p}_\perp}(\mathbf{G}\in\Lambda), \qquad (6)$$

where $M_{\mathbf{p}_\perp}$ is the infinite matrix

$$M_{\mathbf{p}_\perp}=\left\|\frac{1}{2m\gamma}\left|\mathbf{p}_\perp+\mathbf{G}\right|^2\delta_{\mathbf{G},\mathbf{G}'}+V_{\mathbf{G}-\mathbf{G}'}\right\| \quad (\mathbf{G},\mathbf{G}'\in\Lambda) \qquad (7a)$$

and $C_{\mathbf{p}_\perp}$ a column eigenvector:

$$C_{\mathbf{p}_\perp}=[C_{\mathbf{p}_\perp}(\mathbf{G})] \quad (\mathbf{G}\in\Lambda). \qquad (7b)$$

As is well known, $M_{\mathbf{p}_\perp}$ has a denumerably infinite number of eigenvalues for each $\mathbf{p}_\perp$ that are generally nondegenerate. We denote them by $E_\perp^{(n)}(\mathbf{p}_\perp)$ $(n=1,2,...)$ and the corresponding eigenvectors by $C_{\mathbf{p}_\perp}^{(n)}=[C_{\mathbf{p}_\perp}^{(n)}(\mathbf{G})]$ [20]. The diagonalization of $M_{\mathbf{p}_\perp}$ can be effected to a high degree of accuracy by using readily available linear algebra computer packages, after a suitable truncation [21]. The Fourier coefficients $C_{\mathbf{p}_\perp}^{(n)}(\mathbf{G})$ are normalized in the usual way:

$$\sum_{\mathbf{G}\in\Lambda}|C_{\mathbf{p}_\perp}^{(n)}(\mathbf{G})|^2=1. \qquad (8)$$

We also note that the existence of a planar channeling regime for ϕ sufficiently large (but with $\phi,\psi\ll 1$) entails that the transverse eigenvalues $E_\perp^{(n)}(\mathbf{p}_\perp)$ are approximately of the form

$$\frac{1}{2m\gamma}p_\perp^2+e^{(n)}(p_y)\cong\frac{1}{2m\gamma}p^2\phi^2+e^{(n)}(p\psi) \qquad (9)$$

at each such ϕ and ψ, where $p=|\mathbf{p}|$. Here $e^{(n)}(p_y)$ is the eigenvalue of the one-dimensional Hamiltonian [9]

$$\hat{H}=\frac{-1}{2m\gamma}\frac{\partial^2}{\partial y^2}+\hat{V}(y), \qquad (10)$$

indexed by the quasimomentum p_y in the relevant one-dimensional extended-zone scheme. This Hamiltonian governs the motion in the y direction of a relativistic electron with $\mathbf{p}$ almost parallel to the z axis, which has been channeled by the atomic planes parallel to the x,z plane. In Eq. (10), $\underline{V}(y)$ is a one-dimensional potential obtained by averaging $V(x,y)$ over the x axis. The $e^{(n)}(p_y)$'s with the largest populations are those corresponding to ''bound'' states of $\hat{H}$, i.e., those in narrow energy bands of $\hat{H}$ (and hence depending only weakly on p_y).

Let a photon of momentum $\mathbf{k}$, polarized in the direction of the unit vector $\boldsymbol{\epsilon}_\lambda$ ($\lambda=1,2$), be emitted in a spontaneous radiative transition from an initial electronic state $\Psi_i(\mathbf{r})$ to a final state $\Psi_f(\mathbf{r})$. Both of these states are assumed to have the form (1), but of course with the transverse energy $E_\parallel=(p_z^2+m^2)^{1/2}$ for $\Psi_i(\mathbf{r})$ replaced by $E'=(p_z'^2+m^2)^{1/2}$ for $\Psi_f(\mathbf{r})$, and with u replaced by $u^{(n)}_{\mathbf{p}_\perp}(\mathbf{r}_\perp)$, $u^{(n')}_{\mathbf{p}_\perp}(\mathbf{r}_\perp)$, $(n\neq n')$, corresponding to the respective initial and final transverse energies $E_\perp^{(n)}(\mathbf{p}_\perp)$, $E_\perp^{(n')}(\mathbf{p}'_\perp)$. The initial (final) total electron energy $E=E_\parallel+E_\perp^{(n)}(\mathbf{p}_\perp)$ $[E'=E'_\parallel+E_\perp^{(n)}(\mathbf{p}'_\perp)]$ and electron momentum $(\mathbf{p}_\perp,p_z)$ $[p'_\perp,p'_z]$ satisfy the energy-momentum conservation laws

$$E=E'+k, \tag{11a}$$

$$\mathbf{p}_\perp=\mathbf{p}'_\perp+\mathbf{k}_\perp+\mathbf{K}, \quad p_z=p'+k_z. \tag{11b}$$

Here $\mathbf{k}_\perp, k_z$ denote the components of $\mathbf{k}$ respectively perpendicular and parallel to the z axis; $k=|\mathbf{k}|$ is the photon energy; and $\mathbf{K}$, a vector in Λ, is the momentum transferred to the lattice. For the cases of interest in this paper, $k\ll|p_z|$. For these cases Eqs. (11), together with the pertinent definitions, and the periodicity property of the transverse eigenvalues in the present periodic zone scheme [20] entail that the photon energy emitted in the transition is accurately given by the well-known expression

$$k=k_{i\to f}(\theta)=\frac{E_\perp^{(n)}(\mathbf{p}_\perp)-E_\perp^{(n')}(\mathbf{p}_\perp-k_\perp)}{1-\beta_z\cos\theta} \tag{12}$$

in the laboratory frame, where θ is the angle between $\mathbf{k}$ and the z axis, and $\beta_z=p_z/(p_z^2+m^2)^{1/2}$ [22]. Assuming that the incident electron beam is unpolarized, the cross section per unit volume for the production of such a photon, differential with respect to k and the solid angle Ω specifying the direction of photon emission, can be calculated straightforwardly by the approach of Ref. [16] and is given by

$$\frac{1}{v}\frac{d^2\sigma^\lambda_{i\to f}}{dk\,d\Omega}=\frac{1}{2\pi\beta_z}\left(\frac{e}{E}\right)^2\frac{k_{i\to f}(\theta)}{1-\beta_z\cos\theta}\,|C^{(n)}_{\mathbf{p}_\perp}(\mathbf{0})|^2\,\delta(k-k_{i\to f}(\theta))\left|\sum_{\mathbf{G}\in\Lambda}C^{(n)}_{\mathbf{p}_\perp}(\mathbf{G})C^{(n')}_{\mathbf{p}_\perp-\mathbf{k}_\perp}(\mathbf{G})^*[(\mathbf{p}_\perp+\mathbf{G})\cdot\boldsymbol{\epsilon}^\perp_\lambda+p_z\epsilon^z_\lambda]\right|^2, \tag{13}$$

in whose derivation we have also used a familiar property of the Fourier coefficients [20,23]. Here V is the volume of the crystal slab, e the electronic charge, and $\boldsymbol{\epsilon}^\perp_\lambda$ the component of $\boldsymbol{\epsilon}_\lambda$ in the x,y plane. We assume that the vectors $\mathbf{k}$, $\boldsymbol{\epsilon}_1$, $\boldsymbol{\epsilon}_2$ form a right-handed triad and that $\boldsymbol{\epsilon}_1$ lies in the x,z plane, which is parallel to the atomic planes along which the electron is channeled for large enough ϕ. It follows that for the small values of ϕ and ψ considered in this paper $\boldsymbol{\epsilon}_2$ is almost orthogonal to the these planes. Note that $|C^{(n)}_{\mathbf{p}_\perp}(\mathbf{0})|^2$ in Eq. (13) is the population of the initial transverse Bloch state and that the cross section (13) depends implicitly on $\mathbf{K}$ through the indices n,n' of the initial and final Bloch states.

III. RESULTS AND DISCUSSION

The transition region was scanned by performing calculations of photon energy, intensity, and polarization at ϕ values ranging from 10 to 125 mrad. The angle ψ was kept constant throughout the calculations. Since we were primarily interested in studying the transition to planar channeling as ϕ increased, we excluded from our computations the angular region in which essentially pure axial channeling occurs.

Denote by J_λ the coefficient of the delta function in Eq. (13). Then $J_\lambda L$ is the number of photons of polarization $\boldsymbol{\epsilon}_\lambda$ emitted per steradian per incident electron from the crystal in a given direction $\hat{\mathbf{k}}$, where we recall that L denotes the thickness of the crystal slab. For each transition considered, we calculated the photon energy $k_{1\to f}(0)$, intensity J_1+J_2, and polarization $(J_1-J_2)/(J_1+J_2)$ for the case where $\mathbf{k}$ was parallel to the z direction ($\theta=0$) [23]. It was assumed that the temperature of the Si and Ni crystals was 300 K and that their respective Debye temperatures were 543 and 425 K, respectively. We fixed $\psi=1$ mrad in the case of Si and $\psi=0.1°$ in that of Ni. These angles were selected to enable us to compare our results to those found experimentally for these crystals [1–3]. The Si calculations concern the transition from axial channeling in the $\langle 110\rangle$ direction to planar channeling by the (110) planes; those for Ni refer to the transition from $\langle 110\rangle$ axial channeling to (001) planar channeling.

The results of our photon energy, intensity, and polarization calculations for $\theta=0$ in the respective cases of Si and Ni are depicted in Figs. 3 and 4. The numbers used to construct these graphs were obtained by inverting truncated matrices $M_{\mathbf{p}_\perp}$ with 625 rows and columns; i.e., this was the number of Fourier coefficients (beams) in Eq. (5) included in our calculations. Because of the almost endless results obtainable from the diagonalization of such large matrices, it is necessary to impose reasonable restrictions on what one presents graphically. We elected to depict the energy, intensity, and polarization of the *most intense transition* versus ϕ, after subjecting them to a Gaussian averaging process that will be described shortly.

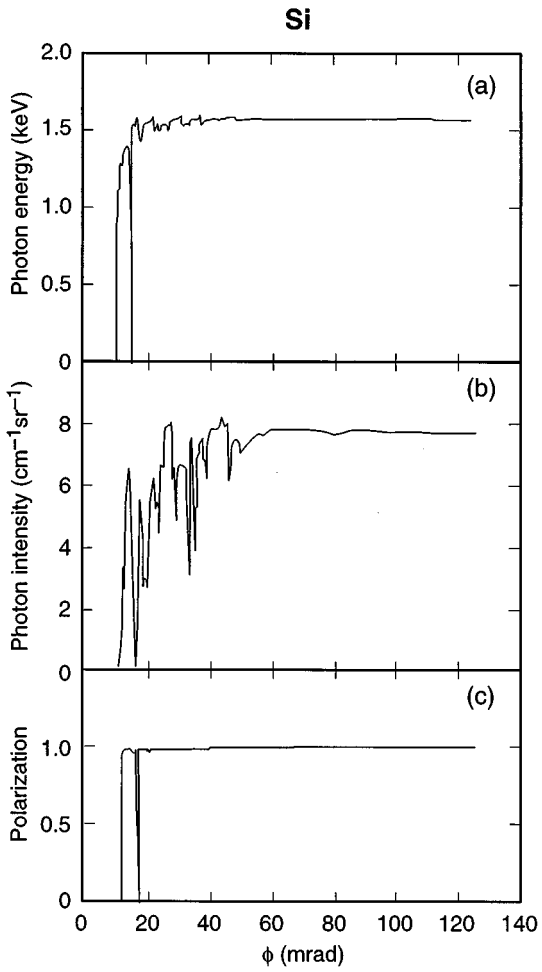

FIG. 3. Calculated properties of CR photons vs ϕ for Si in the axial-to-planar transition region (ψ=1 mrad): (a) laboratory-frame photon energy (keV), (b) intensity (cm^{-1} sr^{-1}), (c) polarization. The graphs in (a)–(c) depict the results obtained by averaging the pertinent numerical data for Si, as described in the text.

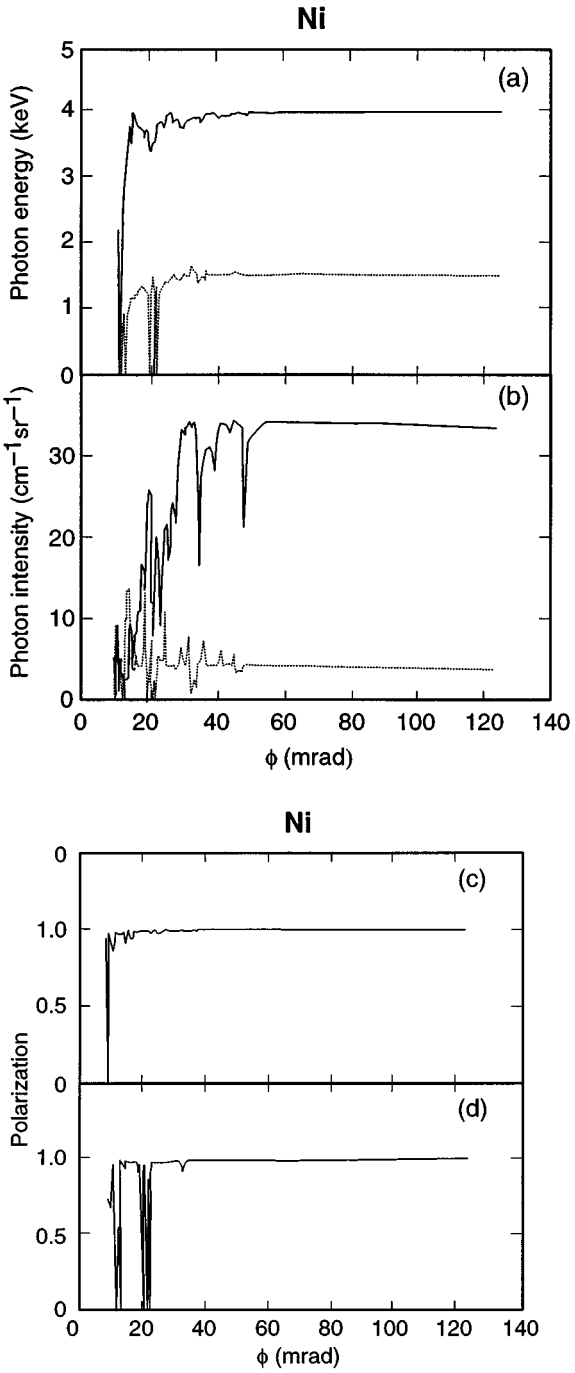

FIG. 4. Calculated properties of CR photons vs ϕ for Ni in the axial-to-planar transition region (ψ=0.1°): (a) laboratory-frame photon energy (keV), (b) intensity (cm^{-1} sr^{-1}), (c) and (d) polarization. The full (dotted) lines in (a)–(d) pertain to the ≈4.1-keV (≈1,6-keV) transitions. The graphs in these figures depict the results obtained by averaging the pertinent numerical data for Ni, as described in the text.

It proved convenient to distinguish two angular regions: (a) $10 \leqslant \phi \leqslant 50$ mrad and (b) $50 < \phi \leqslant 125$ mrad. Because of the rapid variation of the photon intensities with ϕ in region (a), our calculations in this region were performed in steps $\Delta\phi$=0.5 mrad, while in region (b) in which these intensities varied much more slowly, $\Delta\phi$=2 mrad sufficed. The dominating factor controlling the intensities are the populations of the initial levels. At each ϕ considered, we chose the 5–7 most populated levels as initial levels for radiative transitions. For each of these, the top 8–10 transitions were chosen, rejecting photon energies above 10 keV. Finally, from these transitions the 7–9 most intense ones were selected, the larger number being used when ϕ<30 mrad, where the relevant quantities varied most rapidly with ϕ. Inspection of the numerical results revealed local details unsuitable for graphing. For example, on varying ϕ by 0.5 mrad, we sometimes observed an emission ''line,'' which split into two close lines, with approximate conservation of the total intensity. Thus, an averaging of the energies and intensities of lines assuming a Gaussian line shape of relative standard deviation (standard deviation divided by line energy) of 0.085 was made. This width agrees with the linewidth due to finite crystal thickness and instrumental resolution used to fit experimental data of Ref. [3] with Ni [24]. Our graphical results are insensitive to 50% reductions of this width.

We now describe the averaging in region (a) in greater detail, the corresponding averaging in region (b) being the same except for the larger values of $\Delta\phi$ involved. In this process, we began at ϕ=50 mrad and proceeded toward ϕ=10 mrad in $\Delta\phi$=0.5 mrad steps, thus starting from a

region of slow intensity variation and ending up in one of rapid variation. At $\phi=50$ mrad, the mean-energy parameter k_0 of the Gaussian was chosen to be the energy of the most intense line at this angle and a weighted average I_1 of the intensities of the three most intense lines at that angle was computed. The weight of each line was taken to be proportional to the value of the Gaussian at the corresponding photon energy. The mean photon energy k_1 of these three lines was calculated similarly, which differed from k_0 by only a few percent. At the next angular value $\phi=49.5$ mrad considered, the mean-energy parameter of the Gaussian was taken to be k_1. All lines with energies k such that $|k-k_1|\leq 2$ Gaussian half-widths were chosen and the two averaging processes just mentioned were repeated, yielding a mean photon energy k_2 and mean intensity I_2 at this angle. This process was repeated at $\phi=49$ mb, 48.5 mb, etc. At a few low values of ϕ in which the energies of the most intense transitions varied extremely rapidly, no levels were found having energies within the corresponding intervals surrounding the pertinent mean energies, and this led to the zeros shown in the graphs in Figs. 3 and 4. This can be attributed to an overly restricted choice of levels at these low ϕ values and to the fact that the value of $\Delta\phi$ used was too large to capture this rapid variation. Subsequent remarks about the photon energies and intensities should be understood to refer to the respective averaged quantities. On the other hand, the polarization values shown in Figs. 3 and 4 are those of the strongest discrete contributions.

Figure 3(a) shows our results for the energies of emitted photons for Si versus ϕ. These energies exhibit a very fast increase with ϕ in the region $10\leq\phi\leq 15$ mrad, except for a ''dip'' near the end of this interval. They remain constant to within $<10\%$ for $15<\phi\leq 40$ mrad, and are almost flat in the interval $40<\phi\leq 125$ mrad, approaching a value $\cong 1.56$ keV. This value is in good agreement with the measured energy of the photon emitted when an electron channeled by the (110) planes in Si undergoes a $1\rightarrow 0$ transition [14]. Figure 4(a) shows analogous numerical results for Ni. It depicts two photon energies at each of the ϕ values considered. Both of these energies increase very rapidly with ϕ in the region $10\leq\phi\leq 15$ mrad, except for a ''dip'' near 15 mrad. The larger of these energies oscillates by about 15% in the interval $15\leq\phi\leq 40$ mrad and by roughly 3% above 40 mrad, and approaches an ''asymptotic'' value $\cong 3.96$ keV. The lower-energy branch undergoes even more pronounced oscillations for $10\leq\phi\leq 30$ mrad, becoming essentially constant in the angular region $\phi>50$ mrad, where it approaches a value $\cong 1.55$ keV. Photons of approximately the latter two energies, emitted by 4-MeV electrons channeled by the (100) planes of Ni, have been observed [25]. The higher-energy CR line corresponds to the $1\rightarrow 0$ radiative transition.

The calculated intensities of the emitted photons for the respective cases of Si and Ni are graphed as functions of ϕ in Figs. 3(b) and 4(b). We see from Fig. 3(b) that for $10\leq\phi\leq 52$ mrad the photon intensity is strongly oscillating, the amplitude of the oscillations being generally much larger than those of the photon energies in Fig. 3(a). It is interesting that the positions of the minima of the intensities coincide with the corresponding ones of the photon energies in Fig. 3(a). In the interval $52<\phi\leq 125$ mrad, the intensity is almost constant. This fact and the essential constancy of the photon energies in this interval indicate that the transition to planar channeling has been basically completed. The calculated intensities for Ni depicted in Fig. 4(b) show a behavior that is qualitatively similar to that in Fig. 3(b). The upper and lower parts of Fig. 4(b) correspond to the 3.96- and 1.55-keV CR lines in Fig. 4(a). The experimental data on CR emitted by 6.8-MeV electrons undergoing the axial-to-planar transition in diamond are in qualitative agreement with the oscillatory behavior of the photon intensities in the transition region predicted by the present calculations [26]. It should also be noted that our predicted ratio of the intensity of the 3.96-keV line to that of the 1.55-keV line is approximately 4:1. Definitive experimental results with which to compare this prediction do not seem to exist at present [27].

The question naturally arises as to the origin of the photon energy and intensity oscillations depicted in Figs. 3 and 4. An examination of our (unaveraged) numerical data shows that the populations of the transverse states change very rapidly with ϕ in the transition regions considered. Typically, as ϕ increases in such regions, the population of one of these states increases considerably as ϕ varies by as little as a milliradian, until it becomes the most populated state, and then decreases equally rapidly, to be succeeded in the leading place by some other level whose population waxes and then wanes just as abruptly, this process being repeated again and again in a highly irregular manner. This behavior produces crossings of the intensities of the transitions originating in states with the largest populations, and leads to the intensity oscillations depicted in Figs. 3 and 4. At sufficiently large values of ϕ, a distinguished pair of levels emerges with energies and populations that are almost independent of this angle. The intensity of the radiative transition between the latter two levels is much larger than that of the other transitions and is essentially ϕ independent as well, thus signaling the passage to the planar channeling regime. A theoretical explanation of these phenomena is not known to the authors. They appear to be manifestations of quantum ''chaos'' of the transverse electron motion and offer an interesting challenge to future experimental and theoretical research (see Ref. [6]).

The polarizations of the emitted photons are displayed in Fig. 3(c) for Si and in Figs. 4(c) and 4(d) for Ni. The latter two figures correspond to the $\approx$4.0- and $\approx$1.6-keV lines in Ni, respectively. From these figures, one immediately sees that for both crystals these photons are planarly polarized to a high degree in almost the entire angular region investigated. In particular, for Si the polarization is at least 97% for $15<\phi\leq 40$ mrad and essentially 100% above 40 mrad. For the $\approx$4.0-keV line of Ni it rapidly increases to 100% in the interval $10\leq\phi\leq 20$ mrad remaining at this value thereafter. A similar remark can be made about the $\approx$1.6-keV line. These results agree with a long-known theoretical prediction [10] recently confirmed experimentally [28] that CR emitted in the forward direction by planarly channeled electrons is 100% polarized. What is surprising about our polarization results is that they predict that almost complete polarization is attained at such low angles, before the transition to the planar channeling regima has been completed.

Since the 81-beam calculations of CR photon energies [3] in the transition region are in relatively good agreement with experiment, the question arises as to how the intensities and energies computed by using such low-order truncations com-

pare with the more accurate results graphed in Figs. 3 and 4. To investigate this matter, we performed 81-beam calculations of these observables for 4-MeV electrons undergoing the axial-to-planar transition in a Ni crystal. When $\phi > 15$ mrad, these calculations led to energy values of the most intense transitions, which differed by a few percent from those obtained in the 625-beam calculations, but the corresponding intensities did not exhibit an oscillatory behavior and for $\phi > 50$ mrad they approached a plateau value $\approx 30\%$ lower than that attained in the 625-beam calculations. It is not surprising that these 81-beam computations failed to reproduce the rapid oscillatory behavior shown in Fig. 4(b), considering the relatively small number of beams (Fourier coefficients) that were used. Qualitatively similar results were obtained from 81-beam calculations for 4-MeV electrons in Si.

IV. SUMMARY

In Sec. III, we have presented numerical results on the energies, intensities, and polarizations of CR photons emitted by 4-MeV electrons incident on Si and Ni crystals in an angular range corresponding to the transition from axial channeling along the $\langle 110 \rangle$ direction to planar channeling by the (110) planes in the first case and from axial channeling along this direction to planar channeling by the (001) planes in the second. These results, obtained by using the harp model and the many-beam formalism, predict a complex oscillatory behavior of these three properties of CR at ϕ values in the transition region, as well as the emergence of the planar CR regime at sufficiently large angles ϕ. Except for the numerical study of CR intensities in Ref. [3], previous treatments [29] have computed the properties of planar CR on the basis of one-dimensional continuum models, thus implicitly *assuming* the occurrence of this transition. We have found that the ϕ dependence of the photon intensity of the strongest line of the CR spectrum provides a more sensitive way to study the completion of the transition to the planar channeling regime than do the photon energy or polarization values. In this regime, our results agree with the available conventional one-dimensional calculations [2] and experimental observations [2,3]. We predict that the radiation is almost 100% planarly polarized, not only at angles ϕ at which the transition to planar channeling is complete, in accordance with experiment [28] and calculations based on a simple one-dimensional model [10], but also at significantly smaller ϕ values at which planar channeling has not yet been completely achieved. These agreements with observation give one confidence that the harp model yields quantitatively reliable predictions of properties of the radiation from relativistic electrons in the axial-to-planar transition region.

ACKNOWLEDGMENTS

One of the authors (R.W.D.) was partially supported by the National Research Council. We wish to thank Dr. W. E. Pickett for helpful remarks. We also acknowledge useful conversations with Dr. V. L. Jacobs, Dr. M. Rosen, and Professor H. Überall. The present work has also been supported by the Office of Naval Research.

[1] For general theoretical and experimental surveys of CR, see J. U. Anderson, E. Bonderup, and E. Lægsgaard in *Coherent Radiation Sources*, edited by A. W. Sáenz and H. Überall, Topics in Current Physics Vol. 38 (Springer-Verlag, Berlin, 1985); B. Berman and S. Datz, *ibid.*; see also Ref. [2].

[2] J. U. Andersen, K. R. Eriksen, and E. Lægsgaard, Phys. Scr. **24**, 588 (1981).

[3] J. U. Andersen, E. Bonderup, E. Lægsgaard, and A. H. Sørensen, Phys. Scr. **28**, 308 (1983).

[4] See, e.g., J. U. Andersen, S. K. Andersen, and W. M. Augustiniak, K. Dan. Vidensk. Selsk. Mat. Fys. Medd. **39** (10) (1977).

[5] E. Diedrich *et al.*, Nucl. Instrum. Methods B **67**, 275 (1992).

[6] This work was carried out by Dr. P. Hoffman Staschek for her Ph.D. dissertation at the Technical University of Darmstadt (1996), under the direction of Professor A. Richter (private communication from Dr. Hoffmann-Staschek).

[7] Ph. Lervig, J. Lindhard, and V. Nielsen, Nucl. Phys. A **96**, 481 (1967) showed this for nonrelativistic particles axially channeled in infinite crystals. For a mathematically rigorous version of this work, see A. Ben Lemlih, Ph.D. thesis, University of New Mexico, 1986 (unpublished).

[8] See the article by A. W. Sáenz and H. Überall in *Coherent Radiation Sources* (Ref. [1]).

[9] M. A. Kumakhov and R. Wedell, Phys. Status Solidi B **84**, 581 (1977).

[10] See A. W. Sáenz, H. Überall, and A. Nagl, Nucl. Phys. A **372**, 90 (1981), where the intensity and polarization of CR emitted by planarly channeled electrons is discussed for a simple continuum model using the Dirac equation.

[11] For results on the polarization of CR from axially channeled electrons obtained by using the Dirac equation and the many-beam approach, see R. Fusina, Radiat. Eff. Defects Solids **122–123**, 329 (1991).

[12] D. M. Bird and B. F. Buxton, Proc. R. Soc. London Ser. A **379**, 459 (1982) first discussed CR from planarly channeled electrons using the Dirac equation and one-dimensional Bloch states.

[13] See, e.g., J. U. Andersen *et al.* in *Coherent Radiation Sources* (Ref. [1]), Sec. 6.5.

[14] See, e.g., J. U. Andersen *et al.* in *Coherent Radiation Sources* (Ref. [1]), Sec. 6.6.

[15] See Ref. [3], Sec. 4.6 for an interesting semiquantitative discussion of the axial-to-planar transition.

[16] A. W. Sáenz, A. Nagl, and H. Überall, Phys. Rev. B **37**, 7238 (1988).

[17] We use units in which $\hbar = c = 1$.

[18] P. A. Doyle and P. S. Turner, Acta Crystallogr. A **24**, 390 (1968).

[19] See, e.g., C. Kittel, *Introduction to Solid State Physics* (Wiley, New York, 1971), pp. 309, 310.

[20] The eigenvalues $E_{\perp}^{(n)}(\mathbf{p}_{\perp})$ are invariant with respect to translations $\mathbf{p}_{\perp} \rightarrow \mathbf{p}_{\perp} + \mathbf{K}_0 (\mathbf{K}_0 \in \Lambda)$. In the more familiar reduced-zone terminology, $E_{\perp}^{(n)}(\mathbf{p}_{\perp})$ is the transverse electronic energy in the

nth band at the reduced value of the quasi-momentum $\mathbf{p}_\perp$, i.e., the part of $\mathbf{p}_\perp$ lying in the first Brillouin zone. We also recall the property $C^{(n)}_{\mathbf{G}+\mathbf{K}_0}(\mathbf{G}-\mathbf{K}_0)=C^{(n)}_{\mathbf{G}}(\mathbf{G})$ of the Fourier coefficients.

[21] The EISPACK routine CHIEV was used to solve the truncated eigenfunction-eigenvalue problem (5).

[22] The calculation of $E_\perp^{(n')}(\mathbf{p}_\perp-\mathbf{k}_\perp)$ is generally more time consuming if $\mathbf{k}_\perp\neq 0$ than if $\mathbf{k}_\perp=0$ ($\theta=0$), since in the former case (12) is an *implicit* equation for k.

[23] It should be noted that if $\theta=0$, then the expression inside the square brackets in the sum over $\mathbf{G}$ in Eq. (13) simplifies to $\mathbf{G}\cdot\boldsymbol{\varepsilon}^\perp_\lambda$. This follows from the fact that the eigenvectors $[C^{(n)}_{\mathbf{p}_\perp}(\mathbf{G})]$, $[C^{(n')}_{\mathbf{p}_\perp}(\mathbf{G})]$ are orthogonal if $n\neq n'$.

[24] See Ref. [3], Sec. 5.2.

[25] See, Ref. [3], Sec. 5.2, and particularly the portion of Fig. 3, p. 325, concerning planar channeling by the (100) plane in Ni.

[26] P. Hoffmann-Staschek (private communication).

[27] See, however, Ref. [25].

[28] The polarization of channeling radiation was investigated experimentally by E. Diedrich *et al.*, Phys. Lett. A **178**, 331 (1993) (planar channeling) and by M. Rzepka *et al.*, Nucl. Instrum. Methods B **90**, 186 (1994) (planar and axial channeling).

[29] See, e.g., Refs. [2] and [10].